THE JOURNAL OF BIOLOGICAL CHEMISTRY VOL. 284, NO. 16, pp. 10315–10323, April 17, 2009

An Increased Flux through the Glucose 6-Phosphate Pool in Enterocytes Delays Glucose Absorption in *Fxr*$^{-/-}$ Mice*[S]

Received for publication, September 22, 2008, and in revised form, February 4, 2009 Published, JBC Papers in Press, February 9, 2009, DOI 10.1074/jbc.M807317200

Theo H. van Dijk[‡1], Aldo Grefhorst[§1,2], Maaike H. Oosterveer[§], Vincent W. Bloks[§], Bart Staels[¶], Dirk-Jan Reijngoud[‡], and Folkert Kuipers[‡§]

From the Departments of [‡]Laboratory Medicine and [§]Pediatrics, Center for Liver Digestive and Metabolic Diseases, University Medical Center Groningen, University of Groningen, 9700 RB Groningen, The Netherlands and [¶]INSERM U545, Institut Pasteur de Lille, University of Lille 2, 1, rue Calmette, BP 245, F-59019 Lille, France

The farnesoid X receptor (FXR) is involved in regulation of bile acid and lipid metabolism. Recently, a role for FXR in control of glucose metabolism became evident. Because FXR is expressed along the length of the small intestine, we evaluated the potential role of FXR in glucose absorption and processing. During intravenous infusion of a trace amount of D-[6,6-$^2H_2$]glucose, a D-[U-^{13}C]glucose-enriched oral glucose bolus was given, and glucose kinetics were determined in wild-type and *Fxr*$^{-/-}$ mice. Compared with wild-type mice, *Fxr*$^{-/-}$ mice showed a delayed plasma appearance of orally administered glucose. Multicompartmental kinetic modeling revealed that this delay was caused by an increased flux through the glucose 6-phosphate pool in enterocytes. Thus, our results show involvement of FXR in intestinal glucose absorption, representing a novel physiological function for this nuclear receptor.

The bile acid-activated farnesoid X receptor (FXR; NR1H4)[3] is a member of the nuclear receptor superfamily that is expressed in liver, adrenals, kidney, small intestine, and colon (1). Through FXR activation in the liver, bile acids induce transcription of the atypical nuclear receptor short heterodimer partner (NR0B2), which, in turn, represses transcription of the *Cyp7a1* gene, encoding the rate-controlling enzyme in bile acid synthesis (2). FXR also suppresses transcription of the gene encoding the hepatobiliary bile acid uptake transporter NTCP (Na^+-taurocholate cotransporting polypeptide; Slc10a1) and induces transcription of genes encoding canalicular bile acid transporters such as the bile salt export pump (ABCB11) and multidrug resistance protein-2 (ABCC2) (see reviews in Refs. 1 and 3). In the intestine of mice, FXR stimulates transcription of the gene encoding the fibroblast growth factor 15 (4). Fibroblast growth factor 15 reduces hepatic bile acid synthesis by repressing *Cyp7a1* transcription in the liver. Apart from its clearly established effects on bile acid synthesis and transport, FXR is involved in the control of lipid and lipoprotein homeostasis. *Fxr*$^{-/-}$ mice have elevated plasma triglyceride and cholesterol levels (5), and FXR activation decreases plasma triglyceride levels in mice (6). FXR negatively controls apoA-I (7) as well as apoCIII expression (6), which contributes to FXR-mediated control of plasma lipid levels.

Recently, a link between FXR and glucose homeostasis has become evident. It was shown that glucose induces hepatic *Fxr* expression in rodent liver, probably via intermediates of the pentose-phosphate pathway (8). Recent publications indicate that FXR plays a role in the regulation of the transcription of various hepatic carbohydrate metabolism-related genes. Activated FXR represses the transcription of gluconeogenic genes, *e.g.* those encoding phosphenolpyruvate carboxykinase, fructose-1,6-biphosphatase-1, and glucose-6-phosphatase (G6PC) *in vitro* (9). *In vivo* experiments showed that *Fxr*$^{-/-}$ mice have a reduced peripheral insulin sensitivity (10, 11) and a reduced hepatic glucose production rate (12).

Intestinal glucose transport is an important determinant of blood glucose levels. After uptake of glucose by the enterocyte, glucose can take either a direct or an indirect pathway through the cell. In the indirect pathway, glucose is phosphorylated by hexokinase 1 or 2 (HK1 or HK2) into glucose 6-phosphate (G6P). The catalytic subunit of glucose-6-phosphatase (G6PC) dephosphorylates G6P and makes glucose available for transport across the basolateral membrane into the portal vein (13, 14). Recent studies revealing the localization of the FXR protein in the absorptive epithelium of the small intestine (15) lead us to determine the physiological impact of intestinal FXR on glucose homeostasis and intestinal glucose absorption. For this, oral D-[U-^{13}C]glucose tolerance tests (OGTT) were performed, and the absorption of glucose from the intestine was calculated in this non-steady-state situation.

EXPERIMENTAL PROCEDURES

Animals—The *Fxr*$^{-/-}$ mice were generated by Deltagen, Inc. (Redwood City, CA) (16). Male 18–21-week-old *Fxr*$^{-/-}$ mice and wild-type littermates were housed in a light- and tempera-

* This work was supported by European Union Hepadip Grant 018734, Dutch Diabetes Foundation Grant 2002.00.041, an unrestricted research grant from Daiichi Sankyo, Inc. (Parsippany, NJ), and Agence Nationale de la Recherche Grants A05056GS, PPV06217NSA, and ANR-06-PHYSIO-027-01 (Project R06510NS).

[S] The on-line version of this article (available at http://www.jbc.org) contains supplemental Table S1.

[1] Both authors contributed equally to this work.

[2] To whom correspondence should be addressed: Laboratory of Pediatrics, Center for Liver Digestive and Metabolic Diseases, University Medical Center Groningen, University of Groningen, P.O. Box 30.001, 9700 RB Groningen, The Netherlands. Tel.: 31-50-361-1261; Fax: 31-50-361-1732; E-mail: A.Grefhorst@med.umcg.nl.

[3] The abbreviations used are: FXR, farnesoid X receptor; EGP, endogenous glucose production; F, fractional contribution to the sampled compartment; G6P, glucose 6-phosphate; G6PC, glucose-6-phosphatase, catalytic subunit; HK, hexokinase; OGTT, oral glucose tolerance test; RaE, rate of appearance of exogenous glucose; RaT, total rate of glucose appearance; SGLT, sodium dependent glucose/galactose transporter; G6Pase, glucose-6-phosphatase.

ture-controlled facility. The animals were fed a commercially available lab chow (RMH-B; Hope Farms BV, Woerden, The Netherlands). All of the experiments were approved by the Ethics Committee for Animal Experiments of the University of Groningen.

Oral Glucose Tolerance Test—After a 9-h fast (11:00 pm to 8:00 am), the mice were given an oral glucose bolus of 5.6 ± 0.2 mmol·kg^{-1} in 0.2 ml of water under light isoflurane anesthesia. Blood glucose levels were determined in 2 μl of blood drawn from the tail with a handheld Lifescan EuroFlash glucose meter (Lifescan Benelux, Beerse, Belgium) at the indicated time points.

A similar experiment was conducted to determine the effect of the OGTT on plasma insulin levels. After a 9-h fast (11.00 pm to 8.00 am), the mice were given an oral glucose bolus of 5.6 ± 0.2 mmol·kg^{-1} in 0.2 ml of water under light isoflurane anesthesia. About 40 μl of blood was collected by orbital bleeding shortly before the oral glucose bolus. In addition, the same amounts of blood were drawn from the tail at the indicated time points after the oral glucose bolus. Plasma insulin levels were measured using a commercially available enzyme-linked immunosorbent assay kit (Mercodia ultrasensitive mouse insulin enzyme-linked immunosorbent assay; Orange Medical, Tilburg, the Netherlands).

Oral D-[U-^{13}C]Glucose Tolerance Test Combined with Continuous D-[6,6-$^{2}H_2$]Glucose Infusion—The mice were equipped with a permanent catheter in the right atrium via the jugular vein (17). The entrance of the catheter was attached to the skull with acrylic glue, and the mice were allowed to recover for a period of at least 5 days. After a 9-h fast (11:00 p.m. to 8:00 a.m.), the mice received a continuous infusion of 4.4 μmol·kg^{-1}·min^{-1} D-[6,6-$^{2}H_2$]glucose (Cambridge Isotope Laboratories, Andover, MA) for 5 h to determine the total rate of glucose appearance. To determine the appearance of intestine-derived glucose, an oral glucose bolus of 11.2 ± 0.2 mmol·kg^{-1} from which 30% was D-[U-^{13}C]glucose (Cambridge Isotope Laboratories) in 0.2 ml of water was given under light isoflurane anesthesia at 2 h after start of the infusion. At indicated time points, the blood glucose levels were determined in 2 μl of blood with a handheld Lifescan EuroFlash glucose meter, and 10 μl of blood spots were taken from the tail on filter paper for analysis of isotopic enrichments (18). At the end of the experiment, the mice were killed by cardiac puncture under isoflurane anesthesia. The blood and livers were collected for further analysis.

Short Term Oral Glucose Tolerance Test—After a 9-h fast (11:00 p.m. to 8:00 a.m.), the mice were either not treated or were given an oral glucose bolus of 11.2 ± 0.2 mmol·kg^{-1} in 0.2 ml of water under light isoflurane anesthesia. After 30 min, the mice were killed by cardiac puncture under isoflurane anesthesia. The blood and livers were collected for further analysis. Small intestines were removed and rinsed with 10 ml of saline and divided into three equal sections. The samples were taken from the very first part of the intestine and from the middle of each intestinal section for measurements of mRNA expression level and metabolite concentrations.

Gas Chromatography-Mass Spectrometry Measurements—The fractional isotopomer distribution measured by gas chromatography-mass spectrometry (m_0–m_6) was corrected for the fractional distribution caused by natural abundance of isotopes by multiple linear regression as described by Lee *et al.* (19) to obtain the excess fractional distribution of mass isotopomers (M_0–M_6) caused by dilution of infused labeled compounds, *i.e.* D-[U-^{13}C]glucose and D-[6,6-$^{2}H_2$]glucose. This distribution was used in the calculations of blood glucose kinetics.

Single-pool, First Order Kinetic Model—The excess fractional distribution of mass isotopomers was used to calculate the first order absorption process in a one-compartment model (20–22) using SAAM-II software (version 1.2.1; SAAM Institute, University of Washington, Seattle, WA). The formulas used to calculate the concentration *versus* time curves, and the kinetic parameters are given in supplemental Table S1.

Calculations of the Glucose Appearance Rates—The total rate of glucose appearance (RaT) in blood was calculated applying a one-compartment model according to Steele (23). At time point t_2 $RaT_{t2} = ((\text{infusion(glc;}M_2) \times M_2(\text{glc})_{\text{infuse}}) - V_s \times ([\text{glc}]_2 + [\text{glc}]_1)/2 \times (M_2(\text{glc})_{\text{blood,2}} - M_2(\text{glc})_{\text{blood,1}})/(t_2 - t_1)))/M_2(\text{glc})_{\text{blood,2}}$. In this equation infusion(glc;M_2) is the infusion rate of the D-[6,6-$^{2}H_2$]glucose; $M_2(\text{glc})_{\text{infuse}}$ is the excess mole fraction of infused D-[6,6-$^{2}H_2$]glucose; V_s is the glucose distribution volume calculated from a pool fraction of 0.48 with a total glucose volume of 0.222 ml·kg^{-1}, resulting in a V_s of 0.48 × 0.222 liters·kg^{-1} (data generated with the single-pool, first order kinetic model; see Table 2); $[\text{glc}]_2$ and $[\text{glc}]_1$ are blood glucose concentrations at time points t_2 and t_1, respectively; $M_2(\text{glc})_{\text{blood,2}}$ and $M_2(\text{glc})_{\text{blood,1}}$ are the excess mole fraction of blood D-[6,6-$^{2}H_2$]glucose at time points t_2 and t_1, respectively. The total glucose volume was calculated in the single-pool, first order kinetic model. The area under the curve was estimated using the trapezoidal rule.

The rate of appearance of exogenous glucose (RaE) was calculated according to Tissot *et al.* (24). At time point t_2 $RaE_{t2} = ((RaT_{t2} \times (M_6(\text{glc})_{\text{blood,2}} + M_6(\text{glc})_{\text{blood,1}})/2) + (V_s \times ([\text{glc}]_1 + [\text{glc}]_2)/2 \times (M_6(\text{glc})_{\text{blood,2}} - M_6(\text{glc})_{\text{blood,1}})/(t_2 - t_1)))/M_6(\text{glc})_{\text{ingested}}$. In this equation $M_6(\text{glc})_{\text{blood,2}}$ and $M_6(\text{glc})_{\text{blood,1}}$ are the excess mole fractions of blood D-[U-^{13}C]glucose at time points t_2 and t_1, respectively; $M_6(\text{glc})_{\text{ingested}}$ is the excess mole fraction of ingested D-[U-^{13}C]glucose. By subtracting this value from the total rate of appearance, the endogenous glucose production (EGP) was calculated (21): EGP = RaT − RaE.

Metabolite Contents and Gene Expression Levels—Hepatic and intestinal G6P and glycogen content were determined as described previously (25, 26). RNA was isolated from liver and intestinal tissue using the TRIzol method (Invitrogen). Using random primers, RNA was converted to cDNA with Moloney murine leukemia virus reverse transcriptase (Roche Applied Science) according to the manufacturer's protocol. The cDNA levels of the genes of interest were measured by reverse transcription-PCR using the ABI Prism 7700 sequence detection system (Applied Biosystems, Foster City, CA). An amount of cDNA equivalent to 20 ng of total RNA was amplified using the qPCR core kit (Eurogentec, Seraing, Belgium) according to the manufacturer's protocol with the appropriate forward and reverse primers (Invitrogen) and a template-specific 3′-6-carboxy-tetramethyl-rhodamine, 5′-6-carboxy-fluorescein-labeled Double Dye Oligonucleotide probe (Eurogentec). Calibration curves were run on serial dilutions of pooled cDNA

TABLE 1

Biometrical parameters of wild-type and *Fxr*$^{-/-}$ mice

Male wild-type and *Fxr*$^{-/-}$ mice were fasted for 9 h. Body weight and blood glucose concentrations were determined before and after fasting. The values are averages ± S.E.; $n = 12$ (wild-types) and $n = 10$ (*Fxr*$^{-/-}$).

	Wild-type mice	*Fxr*$^{-/-}$ mice
Fed body weight (g)	32.8 ± 1.0	33.9 ± 1.0
Fasted body weight (g)	29.9 ± 0.9	30.1 ± 0.9
Weight loss (g)	2.9 ± 0.1	3.8 ± 0.1[a]
Weight loss (%)	8.8 ± 0.3	11.2 ± 0.9[a]
Fed blood glucose (mmol·l^{-1})	9.5 ± 0.6	6.3 ± 0.3[a]
Fasted blood glucose (mmol·l^{-1})	6.4 ± 0.6	5.1 ± 0.5[a]

[a] $p < 0.05$.

solutions as used in the assay. The data were processed using an ABI sequence detector v.1.6.3. in the linear part of the calibration curves. The PCR results were normalized by β-actin RNA levels. Primer and probe sequences of hexokinase 1 (*Hk1*), hexokinase 2 (*Hk2*), *G6pc,* glucose-6-phosphatase, transporter 1 (*G6pt*; *Slc37a4*), and glucose transporter 2 (*Glut2; Slc2a2*) have been published (27–29). For sodium-dependent glucose/galactose transporter 1 (*Sglt1; Slc5a1*), the following primers/probers were used: sense, GTT GGA GTC TAC GCA ACA GCA A; antisense, GGG CTT CTG TGT CTA TTT CAA TTG T; probe, TCC TCC TCT CCT GCA TCC AGG TCG (accession number NM_019810).

Statistics—All of the values are expressed as the means ± S.E. Statistical differences were determined using one-way analysis of variance or Mann-Whitney *U* test (metabolite concentrations and gene expression data). $p < 0.05$ was considered significant.

RESULTS

Fxr$^{-/-}$ *Mice Show an Altered Plasma Glucose Response during an OGTT*—Although fed male *Fxr*$^{-/-}$ mice and wild-type littermates had comparable body weights, there was a small but statistically significant difference in weight loss upon 9 h of fasting between both groups (Table 1). Blood glucose levels were significantly lower in *Fxr*$^{-/-}$ than in wild-type mice, before and after the 9-h fast. Upon the OGTT, the *Fxr*$^{-/-}$ mice had a reduced and delayed increase of blood glucose levels compared with their wild-type controls with constituently higher plasma insulin concentrations (Fig. 1). This difference in blood glucose concentration between the genotypes might be due to the fact that *Fxr*$^{-/-}$ mice have 1) an enhanced glucose disposal rate; 2) a reduced and/or delayed intestinal glucose absorption rate; and/or 3) a stronger reduction of the endogenous glucose production rate upon OGTT. We therefore investigated blood glucose kinetics in more detail in an experiment in which 30% of the oral glucose bolus was substituted by D-[U-^{13}C]glucose. This experiment was performed in combination with a continuous infusion of a trace amount of D-[6,6-$^{2}H_2$]glucose.

Before the start of the D-[U-^{13}C]glucose-containing OGTT, the *Fxr*$^{-/-}$ mice had slightly lower blood glucose levels compared with wild-type mice (Fig. 2*A*). Within 15 min after oral glucose administration, blood glucose levels rose to maximal levels of 19.0 ± 1.3 mmol·liter^{-1} in wild type and to 14.5 ± 1.1 mmol·liter^{-1} in *Fxr*$^{-/-}$ mice. These levels returned to pre-OGTT levels after 90 min. Blood D-[U-^{13}C]glucose *versus* time

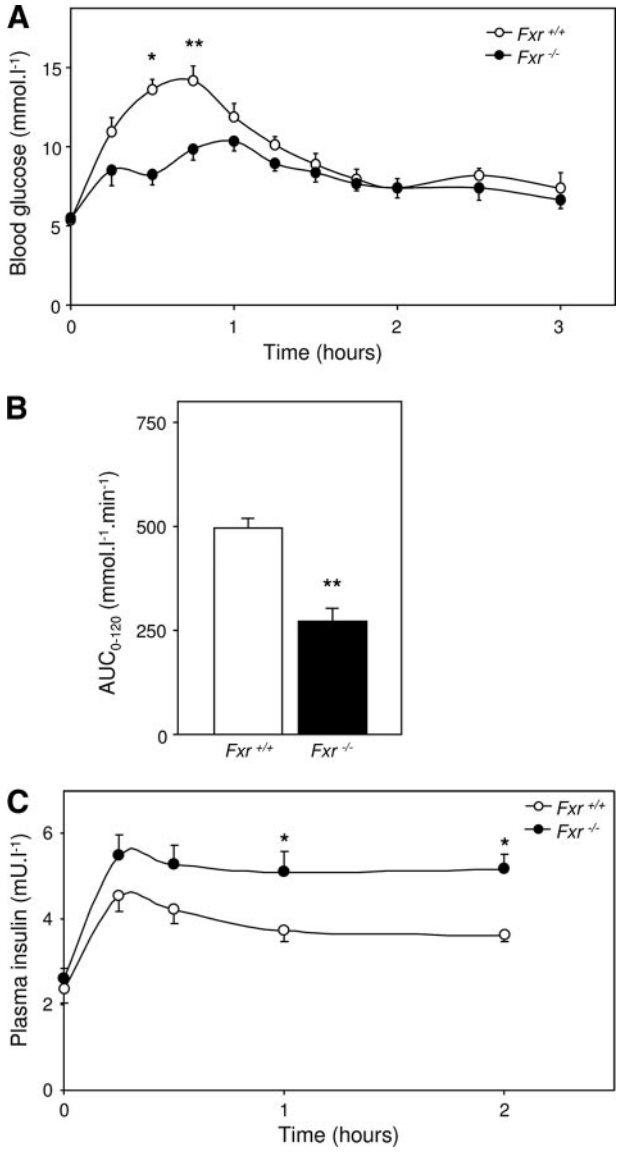

FIGURE 1. **Blood glucose and plasma insulin concentrations during an OGTT.** 9-h fasted male wild-type and *Fxr*$^{-/-}$ mice were subjected to an OGTT (5.6 mmol·kg^{-1}). *A*, blood glucose levels during the OGTT. *B*, the area under curve of the excess of blood glucose level (base line is time point 0 and time points 120–180 min). *C*, plasma insulin levels during the OGTT. The values are averages ± S.E. ($n = 5$). *, $p < 0.05$; **, $p < 0.01$.

curves were different between both groups (Fig. 2*B*). Compared with wild-type mice, D-[U-^{13}C]glucose concentrations were lower in *Fxr*$^{-/-}$ mice during the first 45 min but higher during the last part of the experiment. Applying the formulas for single-pool, first order kinetics (supplemental Table S1), curves were fitted for each individual mouse. Fig. 2*B* shows the averages of data points and estimated curves, whereas the estimated and derived parameters are presented in Table 2.

Extrapolated blood D-[U-^{13}C]glucose concentrations at time 0 (derived from the extrapolation of the elimination period and from extrapolation of the absorption period) were significantly lower in *Fxr*$^{-/-}$ mice compared with wild types. A significantly lower elimination rate constant (k^{el}) was also evident without differences in absorption rate constant (k^{ab}). This observation clearly falsifies the first hypothesis to explain the perturbed

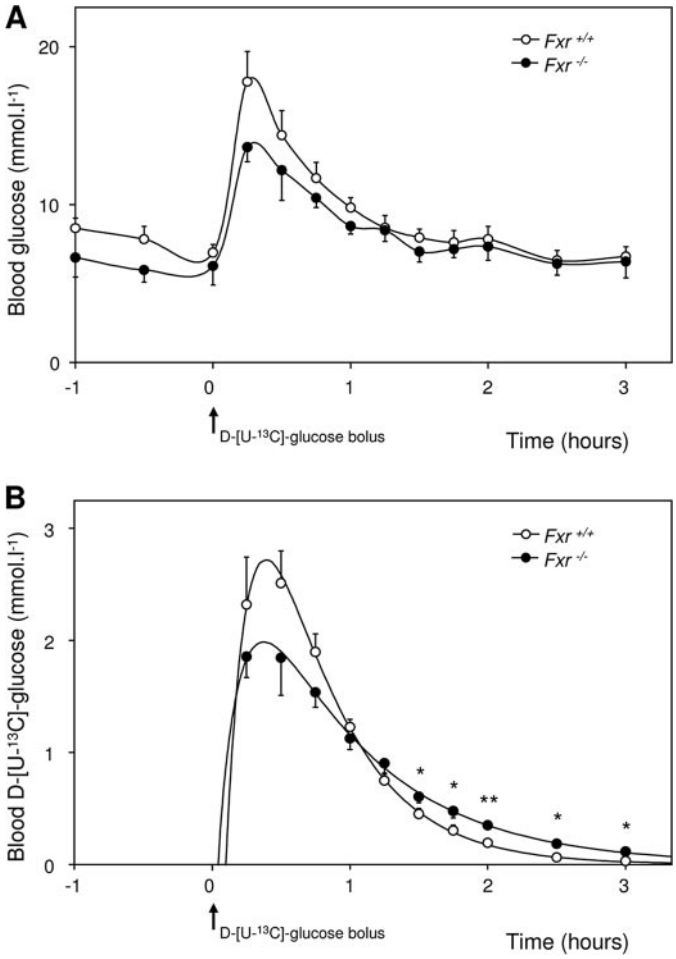

FIGURE 2. **Blood glucose kinetics before and during OGTT using the first order, one-compartment model.** 9-h fasted male wild-type and *Fxr*$^{-/-}$ mice were subjected to an OGTT (11.3 mmol·kg^{-1}, from which 30% was D-[U-^{13}C]glucose) while they were infused with 4.4 μmol·kg^{-1}·min^{-1} D-[6,6-$^{2}H_2$]glucose. *A*, blood glucose concentrations before and during the OGTT. *B*, calculated blood D-[U-^{13}C]glucose concentrations from the fractional contribution of D-[U-^{13}C]glucose with the estimated curve using SAAM II software. The values are averages ± S.E. ($n = 5$). *, $p < 0.05$; **, $p < 0.01$.

blood-glucose curve in *Fxr*$^{-/-}$ mice upon the OGTT. Surprisingly, significantly higher values were calculated for the apparent bioavailability of the oral glucose dose (*F*) in the *Fxr*$^{-/-}$ mice. This higher *F* can be explained by a more gradual introduction of D-[U-^{13}C]glucose into the blood compartment, supporting our second hypothesis: *Fxr*$^{-/-}$ mice have a reduced and/or delayed intestinal glucose absorption.

Fxr$^{-/-}$ *Mice Show Delayed Intestinal Glucose Absorption after an OGTT*—To elucidate why blood glucose levels were markedly less increased after an OGTT in *Fxr*$^{-/-}$ mice, we used non-steady-state equations according to Steele (23).

The continuous infusion of D-[6,6-$^{2}H_2$]glucose enabled us to calculate blood glucose turnover rates during the experiment. *Fxr*$^{-/-}$ mice had a significant reduced base-line glucose turnover compared with wild-type mice (102.4 ± 6.8 *versus* 128.3 ± 8.3 μmol·kg^{-1}·min^{-1}, $p < 0.05$) (Fig. 3*A*). After correction for base-line values (the average from time points −30- 0 and 120–180 min), it was clear that the OGTT-mediated maximal increase of glucose appearance rate was also decreased in *Fxr*$^{-/-}$ mice (185.6 ± 20.1 *versus* 110.8 ± 16.6 μmol·kg^{-1}·min^{-1}, *Fxr*$^{-/-}$ *versus* wild type, $p < 0.05$) (Fig. 3*B*). In addition, the decline of glucose rate of appearance to base-line values was slower in *Fxr*$^{-/-}$ mice.

TABLE 2

Kinetic parameters of ingested D-[U-^{13}C]glucose during the OGTT

9-h fasted male wild-type and *Fxr*$^{-/-}$ mice were subjected to an OGTT (11.3 mmol.kg^{-1}, from which 30% was D-[U-^{13}C]glucose) while they were infused with 4.4 μmol·kg^{-1}·min^{-1} D-[6,6-$^{2}H_2$]glucose. The kinetic parameters were calculated using SAAM II software for curve fitting. D_L, oral dose administrated D-[U-^{13}C]glucose; $C(0)^{el}$, initial D-[U-^{13}C]glucose concentration by extrapolation of elimination period; $C(0)^{ab}$, initial D-[U-^{13}C]glucose concentration by extrapolation of the absorption period; k^{el}, elimination rate constant; k^{ab}, absorption rate constant; t_{lag}, time between administration and appearance of D-[U-^{13}C]glucose in sampled compartment; C_{lag}, concentration at lag time calculated from elimination or absorption curve; t_{max}, time of maximal D-[U-^{13}C]glucose concentration; C_{max}, D-[U-^{13}C]glucose concentration at t_{max}. $t_{½}^{el}$, half-life of blood glucose; MRT, mean residence time of glucose in sampled compartment. *F*, fractional contribution of administrated D-[U-^{13}C]glucose to the sampled compartment; V_D, appearant volume of distribution of administrated D-[U-^{13}C]glucose. The values are averages ± S.E. ($n = 5$).

	Wild-type mice	*Fxr*$^{-/-}$ mice
D_L (mmol·kg^{-1})	3.47 ± 0.09	3.34 ± 0.10
$C(0)^{el}$ (mmol·l^{-1})	9.26 ± 0.44	3.91 ± 0.123[a]
k^{el} (min^{-1})	0.0331 ± 0.0005	0.0201 ± 0.0008[a]
$C(0)^{ab}$ (mmol·l^{-1})	13.16 ± 0.41	4.74 ± 0.24[a]
k^{ab} (min^{-1})	0.091 ± 0.007	0.100 ± 0.007
t_{lag} (min)	6.0 ± 0.4	2.4 ± 0.6[a]
C_{lag} (mmol·l^{-1})	7.60 ± 0.33	3.72 ± 0.13[a]
t_{max} (min)	17.4 ± 0.8	20.1 ± 1.0[b]
C_{max} (mmol.l^{-1})	2.72 ± 0.24	1.99 ± 0.07[b]
$t_{½}^{el}$ (min)	20.9 ± 0.2	34.5 ± 1.2[a]
MRT (min)	41.1 ± 1.0	59.7 ± 1.9[a]
F	0.48 ± 0.04	0.76 ± 0.02[a]
V_D (l·kg^{-1})	0.222 ± 0.016	0.678 ± 0.028[a]

[a] $p < 0.01$.
[b] $p < 0.05$.

Because the oral glucose bolus contained a different stable isotope of glucose than the infusate, we were able to calculate the appearance rate of glucose derived from the intestine. Wild-type mice showed a steep, isolated peak in intestinal glucose absorption, whereas *Fxr*$^{-/-}$ mice showed a blunted absorption rate with a much slower decrease to base line (Fig. 3*C*). In *Fxr*$^{-/-}$ mice, the reduced recovery of intestine-derived glucose in the first 45 min after the oral glucose bolus was fully compensated for in the period thereafter (Fig. 3*D*). Altogether, this resulted in similar recoveries at the end of the test. These data show that *Fxr*$^{-/-}$ mice had delayed but not reduced intestinal glucose absorption after OGTT.

The difference between the total rate of glucose appearance and the appearance of intestine-derived glucose gives the EGP. Base-line EGP was significantly lower in *Fxr*$^{-/-}$ mice than in wild-type mice (Fig. 3*E*). The EGP was significantly reduced in both groups upon administration of the glucose bolus, but the reduction was more pronounced in wild-type mice. The relative reduction was 50 ± 3% *versus* 30 ± 4% in wild-type and *Fxr*$^{-/-}$ mice, respectively. This latter observation of reduced reduction in EGP is inconsistent with our third hypothesis that EGP could be more reduced upon the OGTT in *Fxr*$^{-/-}$ than in wild-type mice.

Reduced Intestinal Glucose Absorbance in Fxr$^{-/-}$ *Mice Is Likely the Result of Increased Glucose Phosphorylation in Proximal Enterocytes*—From the three proposed mechanisms that might explain the delayed increase of blood glucose in *Fxr*$^{-/-}$ mice upon the OGTT, only a delayed intestinal glucose absorption rate seems to be valid. We next tried to unravel the cause of this hampered glucose absorption and tested whether enterocytic glucose handling might be disturbed in *Fxr*$^{-/-}$ mice.

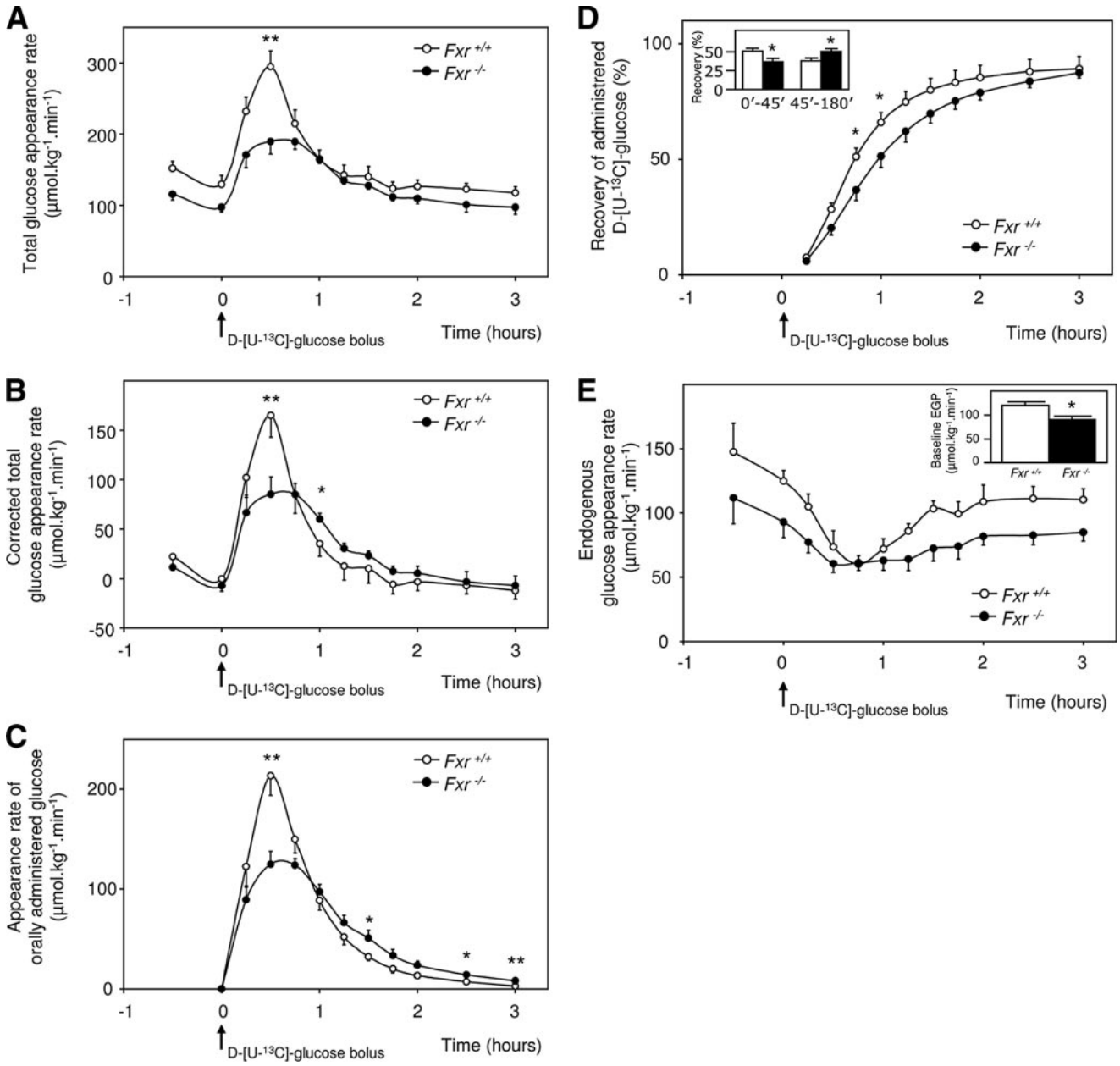

FIGURE 3. **Glucose appearance rates before and during OGTT.** 9-h fasted male wild-type and *Fxr*$^{-/-}$ mice were subjected to an OGTT (11.3 mmol·kg^{-1}, from which 30% was D-[U-^{13}C]glucose) while they were infused with 4.4 μmol·kg^{-1}·min^{-1} D-[6,6-$^{2}H_2$]glucose. *A*, total rate of glucose appearance in blood before and during OGTT. *B*, total rate of glucose appearance in blood before and during OGTT after correction for base-line glucose appearance (base line is time points −1–0 h and 2–3 h). *C*, rate of appearance of orally administrated glucose. *D*, fractional recovery of orally administrated glucose over time with fractional recovery of orally administrated glucose during the first 45 min and during the 45–180 min after oral glucose bolus (*inset*). *E*, endogenous glucose appearance rate with base-line values (*inset*). The values are averages ± S.E. ($n = 5$). *, $p < 0.05$; **, $p < 0.01$.

Therefore, glucose, glycogen, and G6P contents in the liver and small intestine were measured after the absorptive phase of the OGTT. The animals were sacrificed when the blood glucose values reached their peak value (30 min after glucose administration) or at the end of the test (180 min after glucose administration). At both time points hardly any administered glucose was found in the intestinal lumen of both groups, indicating a complete uptake in all mice (Fig. 4*A*). *Fxr*$^{-/-}$ mice had lower hepatic glycogen and G6P contents than wild-type mice 30 min after the oral glucose bolus (Fig. 4, *B* and *C*). In 9-h fasted mice, G6P concentrations in the proximal section of the small intestine were lower in the *Fxr*$^{-/-}$ mice than in wild-type mice (Fig. 4*D*). Enterocyte G6P concentrations were not affected by the OGTT in wild-type mice. In *Fxr*$^{-/-}$ mice, however, they significantly increased to values comparable with that of wild-type mice.

Next, we compared the expression of genes encoding proteins involved in intestinal glucose absorption and metabolism in sequential parts of the small intestine. Expression patterns of the gene encoding the brush border located sodium-dependent glucose/galactose transporter 1 (SGLT1; Slc5A1) and the basolaterally located GLUT2 (glucose transporter-2; Slc2A2) was similar in the *Fxr*$^{-/-}$ and wild-type mice (Fig. 5, *A* and *B*). Compared with wild-type mice, the expression of the genes encoding the glucose-phosphorylating enzymes HK1 and HK2 was

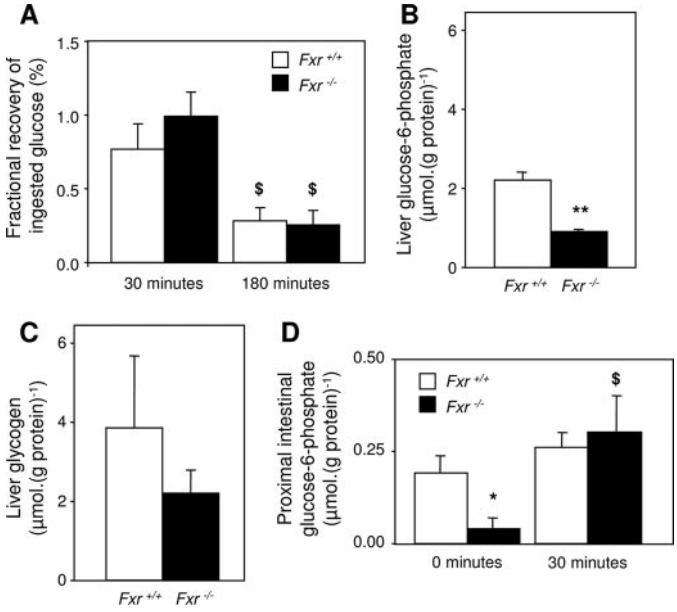

FIGURE 4. **Contents of metabolites in liver and intestine.** 9-h fasted male wild-type and *Fxr*$^{-/-}$ mice were subjected to an OGTT (11.3 mmol·kg^{-1}, from which 30% was D-[U-^{13}C]glucose). *A*, fractional recovery of ingested glucose in the lumen of the small intestine 30 and 180 min after the oral glucose bolus. *B*, hepatic G6P concentration 30 min after the oral glucose bolus. *C*, hepatic glycogen concentration 30 min after the oral glucose bolus. *D*, proximal intestinal G6P concentration 30 min after the oral glucose bolus compared with 9-h fasted mice. The values are averages ± S.E. ($n = 5$). *, $p < 0.05$ between genotypes; **, $p < 0.01$ between genotypes; $, $p < 0.05$ between time points.

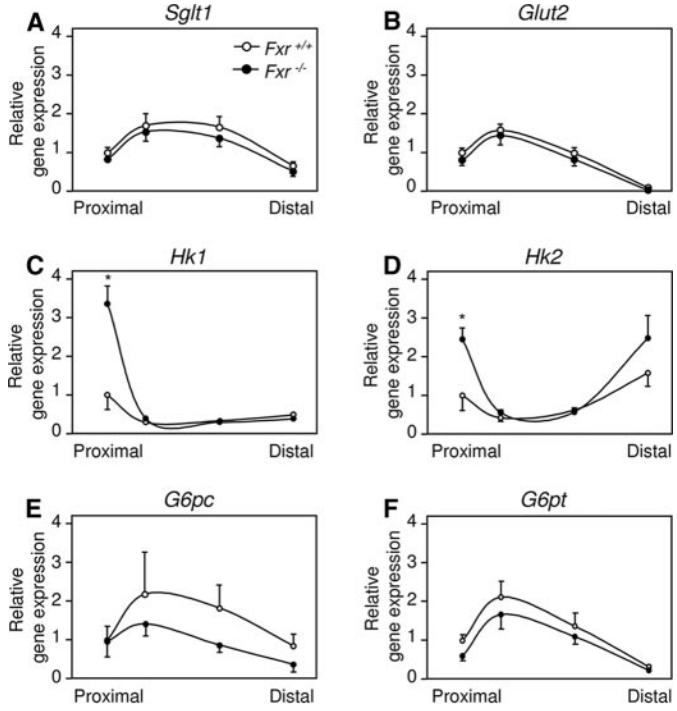

FIGURE 5. **Gene expression profiles of the small intestine.** Gene expressions of enzymes involved in intestinal glucose metabolism in nine-hour fasted male wild-type and *Fxr*$^{-/-}$ mice. Relative mRNA expression was measured by real time PCR as described under "Experimental Procedures." The results are normalized to β-actin and to the most proximal part of the wild-type mice. *Sglt1*, sodium-dependent glucose/galactose transporter-1; *Glut2*, glucose transporter-2; *G6pc*, glucose-6-phosphatase, catalytic subunit; *G6pt*, glucose-6-phosphatase, transporter 1. The values are averages ± S.E. ($n = 5$). *, $p < 0.05$ between genotypes.

significantly increased in the proximal part of the small intestine of *Fxr*$^{-/-}$ mice (Fig. 5, *C* and *D*). Expression of *G6pc* and the gene encoding glucose-6-phosphatase, transporter 1 (*G6pt*; *Slc37a4*) did not differ between both genotypes, although both tended to be lower in *Fxr*$^{-/-}$ mice compared with wild type (Fig. 5, *E* and *F*). Combined, these data suggest that delayed glucose passage through proximal enterocytes of *Fxr*$^{-/-}$ mice is likely the result of an increased glucose phosphorylation.

Diverted Glucose Flux through G6P Pool in Enterocytes of Fxr$^{-/-}$ *Mice*—The metabolic and gene expression data are indicative for an enhanced flux of glucose through G6P in the enterocyte of *Fxr*$^{-/-}$ mice compared with wild-type mice. We therefore considered it feasible to address the process of intestinal glucose absorption using a compartmental model (build using SAAM II software) comprising the direct (without intracellular metabolism) and indirect pathways (comprising the HK and G6Pase reactions) (Fig. 6*A*) as described by Stümpel *et al.* (13). The fit between the simulated appearance of D-[U-^{13}C]glucose in the circulation (Fig. 6*B*) was obtained when the initial direct flux was calculated to be equal to 187 µmol·kg^{-1}·min^{-1} in the wild-type mice and lower (134 µmol·kg^{-1}·min^{-1}) in the *Fxr*$^{-/-}$ mice (Fig. 6*C*). In contrast to the decreased direct flux in *Fxr*$^{-/-}$ mice, the values for the flux through both the HK and G6Pase was increased in the *Fxr*$^{-/-}$ mice. (Fig. 6, *D* and *E*). The sum of the direct and G6Pase fluxes representing the total flux resulted in a glucose flux that is clearly reduced in *Fxr*$^{-/-}$ mice (Fig. 6*F*), especially in the first 30 min after glucose administration. The compartmental model shows that the D-[U-^{13}C]glucose disposal rate was initially lower in *Fxr*$^{-/-}$ mice but was compensated at the end of the experiment (Fig. 6*G*). It can be concluded from this simulation study that in enterocytes of wild-type mice glucose is absorbed preferentially by the direct pathway. In enterocytes of *Fxr*$^{-/-}$ mice, the indirect pathway becomes equally important.

DISCUSSION

FXR is a bile acid-activated nuclear receptor that regulates biosynthesis and enterohepatic transport of bile acids (3, 4). Recently, it was shown that FXR mRNA levels and activity are regulated by glucose (8). In addition, FXR controls expression of several genes encoding enzymes in gluconeogenesis, *e.g. Pck1*, *Fbp1*, and *G6pc* (9). These findings indicate a role for FXR in control of hepatic glucose metabolism, particularly during the fasting-feeding transition (12). Recent reports showed the presence of FXR in the absorptive epithelium of the small intestine (15). The results of the current study clearly show that *Fxr*$^{-/-}$ mice have delayed intestinal glucose absorption caused by an enhanced G6P turnover in the proximal enterocytes. Thus, these results add an extra regulatory role to FXR in the regulation of energy substrate metabolism.

We noticed a difference in blood glucose increase between wild-type and *Fxr*$^{-/-}$ mice during an OGTT (Fig. 1). The increase in blood glucose was clearly delayed in *Fxr*$^{-/-}$ mice, and we therefore speculated that *Fxr*$^{-/-}$ mice might have 1) an enhanced glucose disposal rate; 2) a reduced and/or delayed intestinal glucose absorption rate; and/or 3) a less effective suppression of endogenous glucose production upon OGTT. Accordingly, we decided to analyze intestinal glucose absorp-

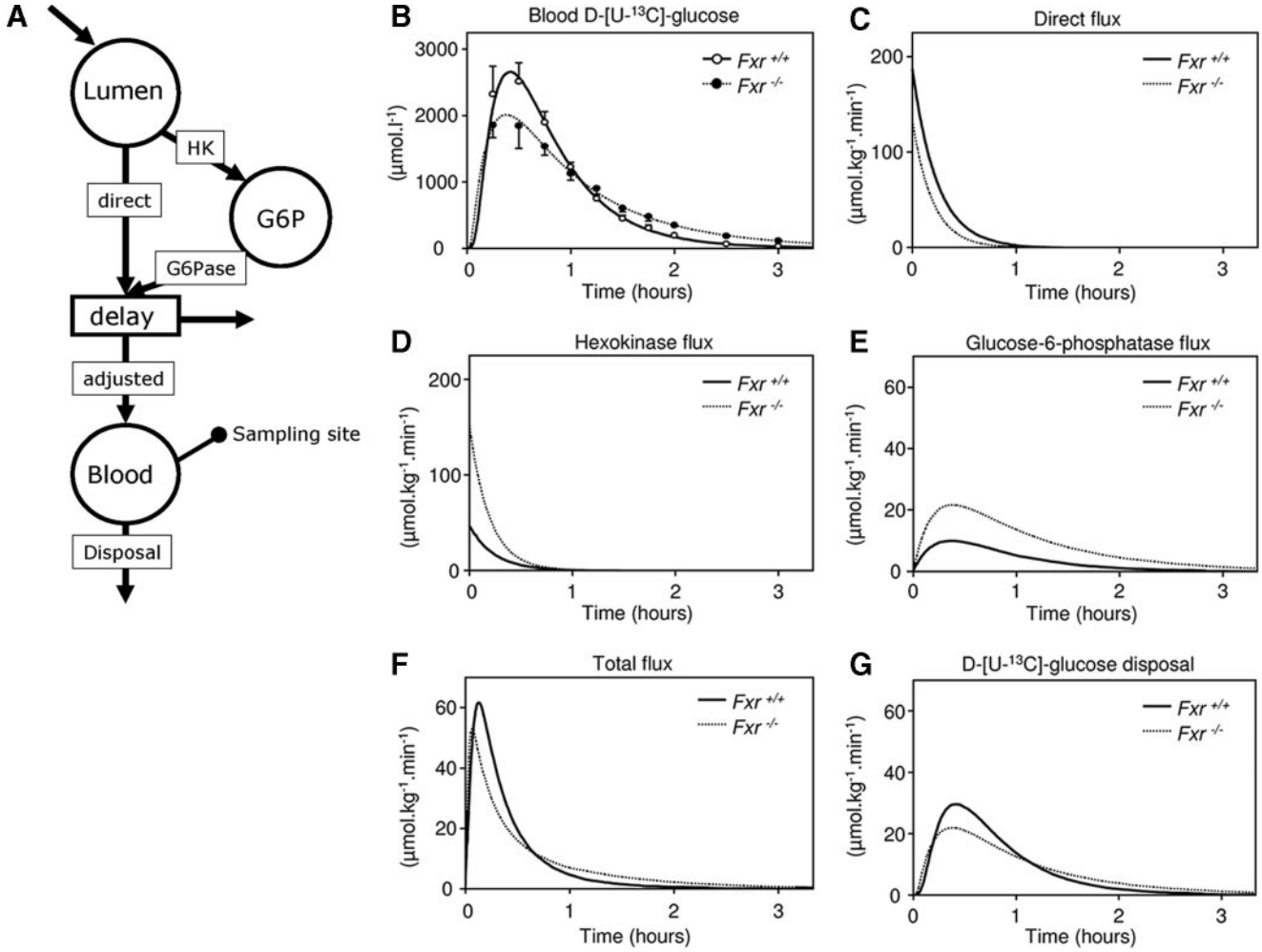

FIGURE 6. **Estimated glucose fluxes during OGTT using compartmental modeling.** 9-h fasted male wild-type and *Fxr*$^{-/-}$ mice were subjected to an OGTT (11.3 mmol·kg^{-1}, from which 30% was D-[U-^{13}C]glucose) while they were infused with 4.4 μmol·kg^{-1}·min^{-1} D-[6,6-$^{2}H_2$]glucose. From the proposed model of glucose metabolism in enterocyte (see Refs. 13 and 14), a compartmental model was made that was used in SAAM II software to calculate fluxes through the compartmental model. *A*, the used compartmental model. The oral bolus was administrated in the intestinal lumen of the mouse. After transport over the brush border membrane the glucose can either leave the enterocyte directly or it is phosphorylated by HKs to G6P. G6P, in turn, can be hydrolyzed in the endoplasmic reticulum to glucose by G6Pase. Both the direct flux and the flux via G6P end in the blood compartment where samples are taken. The amount of glucose ingested has to be corrected to get the amount that enters the sampled pool (*F*). The volume of distribution (V_D) and the lag time (t_{lag}) also have to be known. These three parameters are introduced in the "delay compartment." The used values for these parameters were: $F = 0.48$; $V_D = 0.222$ liters·kg^{-1}; $t_{lag} = 6.0$ min. *B*, calculated concentrations of D-[U-^{13}C]glucose in the sampled pool with the estimated curve. *C*, direct flux from lumen to blood compartment. *D*, hexokinase flux. *E*, glucose-6-phosphatase flux. *F*, flux to the sampled pool after correction for *F*, V_D, and t_{lag}. *G*, flux of D-[U-^{13}C]glucose disposal. The values are averages ($n = 5$).

tion and glucose clearance applying single-pool, first order kinetics to distinguish between these possibilities. Isotopic data were used, obtained by OGTT enriched with D-[U-^{13}C]glucose while the mice were infused with a trace amount of D-[6,6-$^{2}H_2$]glucose before and during the OGTT.

Using the blood D-[U-^{13}C]glucose concentrations solely, glucose absorption and elimination parameters were estimated. The k^{el} was significantly lower in *Fxr*$^{-/-}$ mice. Thus, compared with wild-type mice, *Fxr*$^{-/-}$ mice had a significantly increased blood glucose half-life. Therefore, our first hypothesis to explain the hampered increase in blood glucose upon an oral glucose bolus in *Fxr*$^{-/-}$ mice, *i.e.* an enhanced glucose disposal rate in these mice, has been falsified. Based on earlier work (10), this outcome was expected.

Using both D-[U-^{13}C]glucose and D-[6,6-$^{2}H_2$]glucose data, we were able to calculate glucose turnovers and intestinal glucose absorption under non-steady-state conditions (Fig. 3). Compared with wild type mice, *Fxr*$^{-/-}$ mice had a reduced appearance of glucose in the first 45 min, which was compensated in the period thereafter, resulting in recoveries that were almost the same between both genotypes at the end of the experiment (Fig. 3*D*). This fits with the observation that hardly any glucose was left in the intestinal lumen at 30 and 180 min after oral glucose administration (Fig. 4*A*). These data establish that *Fxr*$^{-/-}$ mice have a delayed but not a decreased glucose appearance rate.

Previously, Cariou *et al.* (12) showed that *Fxr*$^{-/-}$ mice had a reduced EGP compared with wild types, which we could confirm in our experiments (Fig. 3*E*). The data from the current study suggest reduced hepatic insulin sensitivity because the suppression of the EGP upon the OGTT was less pronounced in *Fxr*$^{-/-}$ mice compared with wild-type mice (Fig. 3*E*). Remarkably, the OGTT-mediated reductions of the EGP in *Fxr*$^{-/-}$ and wild-type mice (Fig. 3*E*) were fully comparable with was seen before when hyperinsulinemic euglycemic clamp

experiments were performed (12). We also found a tendency toward increased plasma insulin concentrations in the *Fxr*$^{-/-}$ mice shortly after the OGTT (Fig. 1*C*). For 1 h after the OGTT onwards, the plasma insulin levels were statistically significant increased in the *Fxr*$^{-/-}$ mice. The higher plasma insulin levels of *Fxr*$^{-/-}$ mice (Fig. 1*C*) coincided with lower liver glycogen and liver G6P concentrations (Fig. 4, *B* and *C*), again pointing toward a reduced hepatic insulin sensitivity. In addition, the increased blood glucose mean residence time in the sampled compartment (Table 2) in *Fxr*$^{-/-}$ mice point toward a reduced peripheral insulin sensitivity, as has also been shown before (10, 11). Thus, the current and previous studies (10–12) show reduced hepatic and peripheral insulin sensitivity in *Fxr*$^{-/-}$ mice.

From our initial hypotheses to explain the hampered increase in blood glucose during an OGTT in *Fxr*$^{-/-}$ mice, only a delayed appearance of intestine-derived glucose in *Fxr*$^{-/-}$ mice holds. This delayed appearance can be explained by a delayed glucose transport through the enterocyte and/or enhanced absorption of portal glucose by the liver. The latter is unlikely in view of the reduced hepatic glycogen and G6P concentrations at 30 min after the oral glucose dose (Fig. 4, *B* and *C*). We developed a compartmental model to simulate the consequences of an enhanced glucose metabolism inside enterocytes on the kinetics of glucose absorption. The model was based on the observations published by Stümpel *et al.* (13). They showed that in isolated intestines of *Glut2*$^{-/-}$ mice, addition of the G6Pase inhibitor S4048 almost completely abolished glucose transport across the intestinal wall. Apparently, when the direct transport of glucose across the intestinal wall via SGLT1 and Glut2 is absent, glucose transport proceeds by means of an indirect pathway involving glucose phosphorylation/dephosphorylation inside enterocytes. When this model is applied using our glucose data, it becomes clear that *Fxr*$^{-/-}$ mice have an enhanced flux through the enterocytic G6P pool compared with wild-type mice (Fig. 6, *D* and *F*). An enhanced enterocyte glucose cycling is supported by the observation that the oral glucose administration resulted in a 6-fold increase of G6P in the proximal part of the small intestine in *Fxr*$^{-/-}$ mice, whereas this increase was absent in wild-type mice (Fig. 4*D*). The increased *Hk1* and *Hk2* mRNA levels in the proximal part of the small intestine in *Fxr*$^{-/-}$ mice compared with wild-type mice (Fig. 5, *C* and *D*) also underscore an increased conversion of glucose in G6P in this part of the intestine.

Remarkably, the largest effects of *Fxr* deficiency on gene transcription were found in the very proximal part of the small intestine (Fig. 5, *C* and *D*), the part considered not to contribute to absorption of bile acids secreted into the bile. Therefore the physiological relevance of bile acids in control of intestinal glucose metabolism is unclear and needs more investigation. The role of FXR as a glucose-regulated nuclear transcription factor (8) suggests a physiological function in intestinal glucose absorption. Whether postprandial bile acids activate FXR in proximal small intestine remains to be established. The presence of FXR in tissues that are normally not exposed to bile acids, *e.g.* adipose tissue, adrenal glands, and skin (15), suggests the existence of alternative endogenous FXR ligands.

In conclusion, the experiments described in this paper show that *Fxr*$^{-/-}$ mice have delayed intestinal glucose absorption, supporting a novel regulatory role of FXR in the enterocyte. Once again, these studies show that bile acid, carbohydrate, and lipid metabolism are closely linked. In addition, this paper shows the feasibility of the single pool, first order kinetic model to study kinetics of intestinal glucose absorption and processing with stable isotopes.

Acknowledgments—We thank Rick Havinga, Theo Boer, and Gemma Brufau for skillful technical assistance.

REFERENCES

1. Kuipers, F., Claudel, T., Sturm, E., and Staels, B. (2004) *Rev. Endocr. Metab. Disord.* **5,** 319–326
2. Lu, T. T., Makishima, M., Repa, J. J., Schoonjans, K., Kerr, T. A., Auwerx, J., and Mangelsdorf, D. J. (2000) *Mol. Cell.* **6,** 507–515
3. Chiang, J. Y. (2002) *Endocr. Rev.* **23,** 443–463
4. Inagaki, T., Choi, M., Moschetta, A., Peng, L., Cummins, C. L., McDonald, J. G., Luo, G., Jones, S. A., Goodwin, B., Richardson, J. A., Gerard, R. D., Repa, J. J., Mangelsdorf, D. J., and Kliewer, S. A. (2005) *Cell Metab.* **2,** 217–225
5. Sinal, C. J., Tohkin, M., Miyata, M., Ward, J. M., Lambert, G., and Gonzalez, F. J. (2000) *Cell* **102,** 731–744
6. Claudel, T., Inoue, Y., Barbier, O., Duran-Sandoval, D., Kosykh, V., Fruchart, J., Fruchart, J. C., Gonzalez, F. J., and Staels, B. (2003) *Gastroenterology* **125,** 544–555
7. Claudel, T., Sturm, E., Duez, H., Torra, I. P., Sirvent, A., Kosykh, V., Fruchart, J. C., Dallongeville, J., Hum, D. W., Kuipers, F., and Staels, B. (2002) *J. Clin. Investig.* **109,** 961–971
8. Duran-Sandoval, D., Mautino, G., Martin, G., Percevault, F., Barbier, O., Fruchart, J. C., Kuipers, F., and Staels, B. (2004) *Diabetes* **53,** 890–898
9. Yamagata, K., Daitoku, H., Shimamoto, Y., Matsuzaki, H., Hirota, K., Ishida, J., and Fukamizu, A. (2004) *J. Biol. Chem.* **279,** 23158–23165
10. Cariou, B., van Harmelen, K., Duran-Sandoval, D., van Dijk, T. H., Grefhorst, A., Abdelkarim, M., Caron, S., Torpier, G., Fruchart, J. C., Gonzalez, F. J., Kuipers, F., and Staels, B. (2006) *J. Biol. Chem.* **281,** 11039–11049
11. Ma, K., Saha, P. K., Chan, L., and Moore, D. D. (2006) *J. Clin. Investig.* **116,** 1102–1109
12. Cariou, B., van Harmelen, K., Duran-Sandoval, D., van Dijk, T., Grefhorst, A., Bouchaert, E., Fruchart, J. C., Gonzalez, F. J., Kuipers, F., and Staels, B. (2005) *FEBS Lett.* **579,** 4076–4080
13. Stümpel, F., Burcelin, R., Jungermann, K., and Thorens, B. (2001) *Proc. Natl. Acad. Sci. U. S. A* **98,** 11330–11335
14. Uldry, M., and Thorens, B. (2004) *Pfluegers Arch. Eur. J. Physiol.* **447,** 480–489
15. Higashiyama, H., Kinoshita, M., and Asano, S. (2008) *Acta Histochem.* **110,** 86–93
16. Kok, T., Hulzebos, C. V., Wolters, H., Havinga, R., Agellon, L. B., Stellaard, F., Shan, B., Schwarz, M., and Kuipers, F. (2003) *J. Biol. Chem.* **278,** 41930–41937
17. Kuipers, F., Havinga, R., Bosschieter, H., Toorop, G. P., Hindriks, F. R., and Vonk, R. J. (1985) *Gastroenterology* **88,** 403–411
18. van Dijk, T. H., Boer, T. S., Havinga, R., Stellaard, F., Kuipers, F., and Reijngoud, D. J. (2003) *Anal. Biochem.* **322,** 1–13
19. Lee, W. N., Byerley, L. O., Bergner, E. A., and Edmond, J. (1991) *Biol. Mass. Spectrom.* **20,** 451–458
20. Cobelli, C., Mari, A., and Ferrannini, E. (1987) *Am. J. Physiol.* **252,** E679–E689
21. Mari, A. (1992) *Am. J. Physiol.* **263,** E400–E415
22. Proietto, J., Rohner-Jeanrenaud, F., Ionescu, E., Terrettaz, J., Sauter, J. F., and Jeanrenaud, B. (1987) *Am. J. Physiol.* **252,** E77–E84
23. Steele, R. (1959) *Ann. N. Y. Acad. Sci.* **82,** 420–430
24. Tissot, S., Normand, S., Guilluy, R., Pachiaudi, C., Beylot, M., Laville, M., Cohen, R., Mornex, R., and Riou, J. P. (1990) *Diabetologia* **33,** 449–456
25. Hohorst, H. J. (1970) in *Methoden der Enzymatischen Analyse* (Bergmeyer, H. U., ed) pp. 1200–1204, Verlag Chemie, Weinheim, Germany

26. Keppler, D., and Decker, K. (1970) in *Methoden der Enzymatischen Analyse* (Bergmeyer, H. U., eds) pp. 1089–1094, Verlag Chemie, Weinheim, Germany
27. Grefhorst, A., van Dijk, T. H., Hammer, A., van der Sluijs, F. H., Havinga, R., Havekes, L. M., Romijn, J. A., Groot, P. H., Reijngoud, D. J., and Kuipers, F. (2005) *Am. J. Physiol.* **289,** E829–E838
28. Bandsma, R. H., Grefhorst, A., van Dijk, T. H., van der Sluijs, F. H., Hammer, A., Reijngoud, D. J., and Kuipers, F. (2004) *Diabetologia* **47,** 2022–2031
29. van der Leij, F. R., Bloks, V. W., Grefhorst, A., Hoekstra, J., Gerding, A., Kooi, K., Gerbens, F., te Meerman, G., and Kuipers, F. (2007) *Genomics* **90,** 680–689